CORE
Metadata, citation and similar papers at core.ac.uk
Provided by PolyU Institutional Repository

Fusion Splicing Photonic Crystal Fibers and Conventional Single-Mode Fibers: Microhole Collapse Effect

Limin Xiao, *Student Member, OSA*, M. S. Demokan, *Senior Member, IEEE*, Wei Jin, *Senior Member, IEEE, Member, OSA*, Yiping Wang, and Chun-Liu Zhao

***Abstract*—We investigate the microhole collapse property of different photonic crystal fibers (PCFs) and its effect on the splice loss using an electric arc fusion splicer. The physical mechanism of the splice loss for different kinds of PCFs is studied, and a guideline for splicing these PCFs and conventional single-mode fibers (SMFs) is proposed. We demonstrate a low-loss fusion splicing of five different PCFs with SMFs, including large-mode PCF, hollow-core PCF, nonlinear PCFs, and polarization-maintaining PCF.**

***Index Terms*—Fusion splicing fibers, micro-optical devices, microstructure fabrication, photonic crystal fiber.**

I. Introduction

PHOTONIC crystal fibers (PCFs), which are also called microstructured optical fibers or holey fibers, have been investigated with great interest and have considerably altered the traditional fiber optics [1]–[3] since they appeared in the mid 1990s [4]. PCFs have a periodic array of microholes that run along the entire fiber length. They typically have two kinds of cross sections: One is an air–silica cladding surrounding a solid silica core, and the other is an air–silica cladding surrounding a hollow core. The light-guiding mechanism of the former is provided by means of a modified total internal reflection (index guiding), while the light-guiding mechanism of the latter is based on the photonic bandgap effect (PBG guiding). Because of their freedom in design and novel wave-guiding properties, PCFs have been used for a number of novel fiber-optic devices and fiber-sensing applications that are difficult to be realized by the use of conventional fibers. PCFs will have a great potential for commercial products in many applications in the next decade [3].

To realize the full potential of PCFs, it is necessary to efficiently couple light from conventional single-mode fibers (SMFs) to PCFs. However, because PCFs have microhole structures that are totally different from conventional fibers, splicing different PCFs to conventional fibers is a significant challenge. The microhole collapse phenomenon and its effect on splice loss is a new issue that is very important to the understanding of splice loss. To explore novel splice methods between these different types of fibers, a systematic investigation needs to be conducted, which has not been done so far.

Since Bennett *et al.* [5] first reported experimentally splicing SMFs and PCFs in 1999, many splice methods have been proposed for PCFs. One solution is to design special solid-core PCFs that have the same mode field diameters (MFDs) as SMFs [6], [7] or to design PCFs with a doped core [8], [9] that will guide light even when the air holes have completely collapsed during splicing. However, those methods will limit the flexibility in PCF designs. For solid-core PCFs and SMFs having similar MFDs, low-loss splices were achieved by using fusion splicers [5], [10], [11] or CO_2 lasers [12], [13]. Another type of low-loss high-strength splice between a solid-core PCF and an SMF having similar MFDs was achieved by using a gradient-index fiber lens [14]. For hollow-core PCFs and SMFs having similar MFDs, low-loss splices were reported by using fusion splicers [15]–[17]. For small-core PCFs and SMFs, several indirect splicing methods have been proposed, such as tapered intermediate PCFs [18], [19], integrating an SMF with a PCF during the manufacturing stage of the PCF [20], and using microtips [21]. Recently, we proposed a method of low-loss splicing small-core PCFs and SMFs directly using repeated arc discharges [22].

Because the splicing problem between PCFs and SMFs is still a major limitation that hinders the incorporation of PCFs into conventional fiber systems, it is very important to find a simple and low-cost way to splice different PCFs with conventional SMFs. Since fusion splicing is the most mature technology in splicing fibers and commercial fusion splicers are widely used, it will be a simple and practical solution to splice SMFs and PCFs. However, fusion splicers are mostly reported for use in splicing SMFs and PCFs having similar MFDs, and fusion splicers from different companies or different types have different parameter sets. Therefore, the value of the optimized parameters will be limited for splicing fibers with different structures.

In this paper, we investigate the nature of microhole collapse when splicing and its effect on splicing loss. Different kinds of

Manuscript received April 28, 2007; revised July 30, 2007. This work was supported in part by the Hong Kong SAR Government under Competitive Earmarked Research Grant PolyU 5243/04E.

L. Xiao, M. S. Demokan, W. Jin, and Y. Wang are with the Department of Electrical Engineering, Hong Kong Polytechnic University, Kowloon, Hong Kong (e-mail: xiaolimin.ee@polyu.edu.hk; demsdemo@inet.polyu.edu.hk; eewjin@polyu.edu.hk; ypwang@polyu.edu.hk).

C.-L. Zhao was with the Department of Electrical Engineering, Hong Kong Polytechnic University, Kowloon, Hong Kong. She is now with the School for Information and Optoelectronics Science and Engineering, South China Normal University, Guangzhou 510631, China (e-mail: zhchunliu@hotmail.com).

Color versions of one or more of the figures in this paper are available online at http://ieeexplore.ieee.org.

Digital Object Identifier 10.1109/JLT.2007.907787

0733-8724/$25.00 © 2007 IEEE

Authorized licensed use limited to: IEEE Xplore. Downloaded on October 22, 2008 at 22:10 from IEEE Xplore. Restrictions apply.

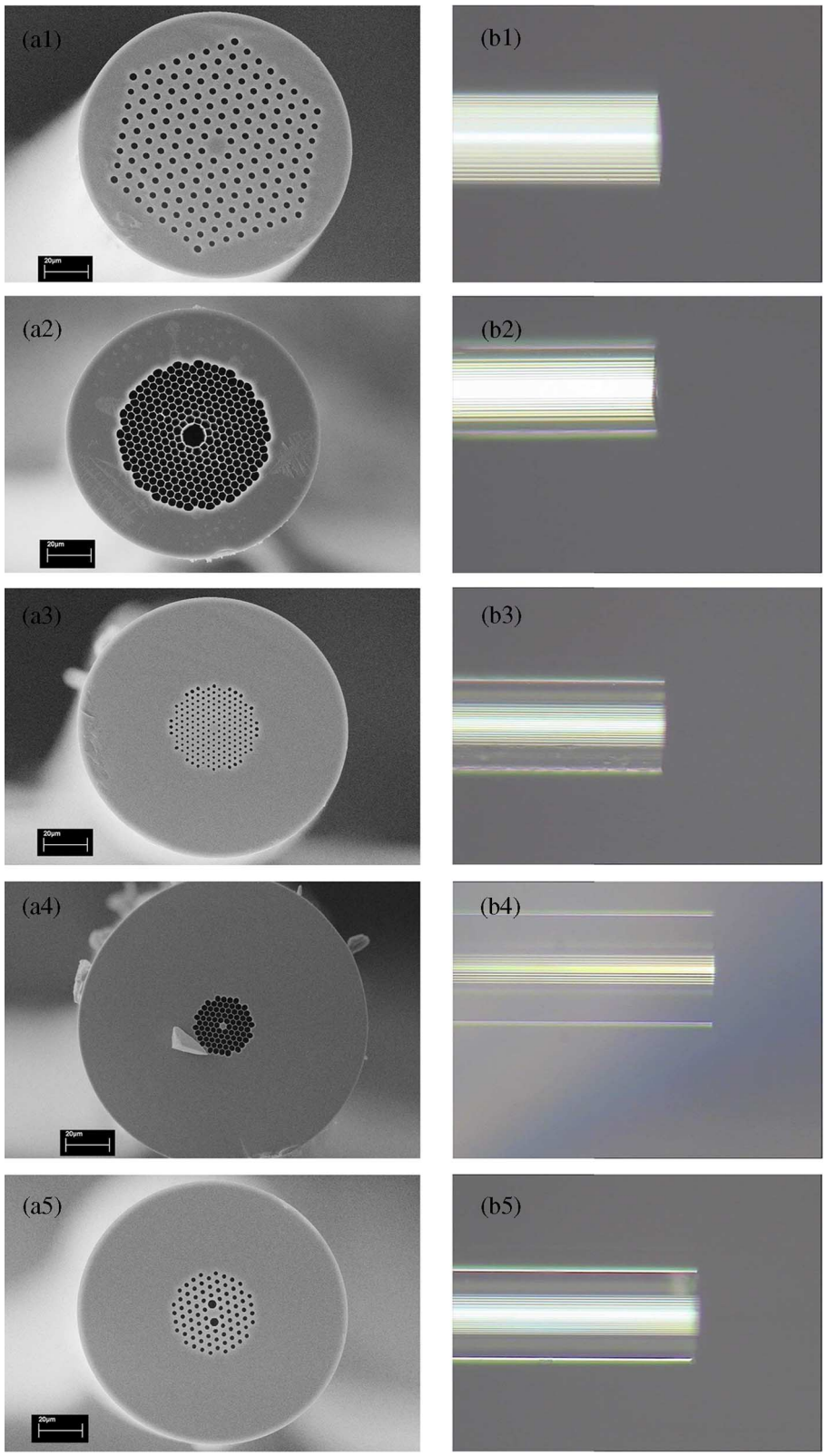

Fig. 1. SEM images of the cross section of the different PCFs used for the experiments. (a1) LMA-10, (a2) HC-1550-02, (a3) LMA-5, (a4) NL-3.3-880, and (a5) PM-1550-01. Optical microscope image of the side view of the corresponding PCFs used for the experiments. (b1) LMA-10, (b2) HC-1550-02, (b3) LMA-5, (b4) NL-3.3-880, and (b5) PM-1550-01.

PCFs have different microhole structures, and the properties of heat-induced collapse when splicing are quite different. One solution that is suitable for one kind of PCF will fail when it is applied to other kinds of PCF. So a detailed study about the effect of microhole collapse on the splice loss for different kinds of PCFs is very important, which clearly and visually explains the

Authorized licensed use limited to: IEEE Xplore. Downloaded on October 22, 2008 at 22:10 from IEEE Xplore. Restrictions apply.

TABLE I
FIBER PARAMETERS AT 1550 nm

Fiber	Core diameter (μm)	Relative hole size d/Λ	Pitch Λ (μm)	MFD (μm)	Numerical aperture (NA)
LMA-10	10.71	0.46	7.14	8.5	0.14
HC-1550-02	10.9	>90%*	3.8	7.5	0.12
LMA-5	4.5	0.44	2.9	4.1	0.23
NL-3.3-880	3.4	>89%*	3.0	2.2	0.41
PM-1550-01	—	Large hole 0.97 Small hole 0.51	4.17	Long axis 3.6 Short axis 3.1	—
SMF-28	8.3	—	—	10.4	0.14

* Air filling fraction

physical mechanism of the splice loss and helps us to find the best way to splice different PCFs. Also, the optimized parameters corresponding to the status of microhole collapse are valuable for users in finding the optimized values when using other splicers. In this paper, we provide the guidelines and demonstrate the simple techniques for low-loss splicing five different kinds of PCFs with SMFs using a conventional fusion splicer.

II. CHALLENGES IN SPLICING PCFs AND SMFs

The splice loss is generally due to two reasons: one is the mode field mismatch between PCFs and SMFs, and the other is that the air holes in PCFs may completely collapse in the vicinity of the splice joint during the splicing process, which significantly increases the coupling loss by destroying the light-guiding structure of the PCF near the joint interface.

In this paper, we investigated the splicing of five different PCFs with conventional SMFs. The PCFs are LMA-10, HC-1550-02, LMA-5, NL-3.3-880, and PM-1550-01 from Crystal-Fiber A/S, as shown in Fig. 1. Fig. 1(a) shows scanning electron microscope (SEM) micrographs of these PCF cross sections, and Fig. 1(b) shows side views of these PCFs through an optical microscope. We can observe the microhole channels from the side views, which will be of benefit in determining the degree of collapse of the air holes after fusion splicing in our experiments. The conventional SMF used in our experiments is SMF-28 from Corning. The fiber parameters are listed in Table I. An Ericsson FSU-975 fusion splicer was used in the experiments.

A. Collapse of Air Holes

When fusion splicing conventional fibers, the fiber tips are heated above the softening point and are then pressed together to form a joint. However, when the temperature of heated PCFs exceeds the softening point, the surface tension will overcome the viscosity and cause the PCF's cylindrical air holes to collapse. Further, the softening point of the PCFs is in general lower than that of SMFs because PCFs have a smaller average solid silica diameter (due to air–silica structures) than that of conventional SMFs [13], assuming that the heat absorption coefficient is almost the same for PCFs and SMFs. The rate

Fig. 2. Side views of the splicing joint on the screen of the FSU-975 splicer using the program set for conventional SMFs when HC-1550-02 is spliced to SMF-28.

TABLE II
COMPARISON OF CONNECTION LOSSES FROM SMF TO DIFFERENT PCFs

Splice type	Theoretical estimation loss (dB)	Butt-coupling loss (dB)	Optimized splice loss (dB)
SMF-28/LMA-10	0.18	0.41	0.19
SMF-28/HC-1550-02	0.46	1.50	1.45
SMF-28/LMA-5	3.32	3.62	0.90
SMF-28/NL-3.3-880	7.85	8.14	2.53
SMF-28/PM-1550-01	4.70	4.88	2.03

of air hole collapse can be given by [14], [23]

$$V_{\text{collapse}} = \frac{\gamma}{2\eta} \tag{1}$$

where γ is the surface tension, and η is the viscosity. The surface tension of silica is not very sensitive to temperature over the range encountered in splicing, but the viscosity of silica sharply decreases with increasing temperature, so the rate of the air hole collapse increases with temperature. If we use the program that is set for conventional SMFs, the total arc discharge energy is too high for a PCF so that the applied heat will collapse the air holes of the PCF completely at the joint part. This causes the splice loss to become very large because the waveguide structure of the PCF near the splice joint is destroyed. For the PCFs (LMA-10, LMA-5, NL-3.3-880, and PM-1550-01), the length of the collapsed region is about 600 μm, so the light will significantly expand due to the disappearance of the difference between the refractive indices of the core and the cladding, thus causing a huge splice loss. The splice losses measured were, respectively, 10.73, 20.11, 21.56, and 25.78 dB for SMF-28/LMA-10, SMF-28/LMA-5, SMF-28/NL-3.3-880, and SMF-28/PM-1550-01 at 1550 nm. In the case of SMF-28/HC-1550-02, the splicing joint could not even be formed because of serious collapsing due to excessive heating to HC-1550-02, as shown in Fig. 2. Therefore, it is very important to avoid serious collapse of air holes when fusion splicing PCFs and SMFs.

B. Mode Field Mismatch

The butt-coupling loss α between PCF and SMF in an optimal alignment can be approximately expressed by [13], [17]

$$\alpha = -20\log\left(\frac{2\omega_{\text{PCF}}\omega_{\text{SMF}}}{\omega_{\text{PCF}}^2 + \omega_{\text{SMF}}^2}\right) \tag{2}$$

where $2\omega_{\text{PCF}}$ and $2\omega_{\text{SMF}}$ are the MFDs of the PCF and SMF, respectively. The butt-coupling loss for light propagating from SMF to PCF was experimentally measured at 1550 nm. The butt-coupling losses agree well with the theoretical estimation given in (2), as shown in Table II. The good agreement between

Authorized licensed use limited to: IEEE Xplore. Downloaded on October 22, 2008 at 22:10 from IEEE Xplore. Restrictions apply.

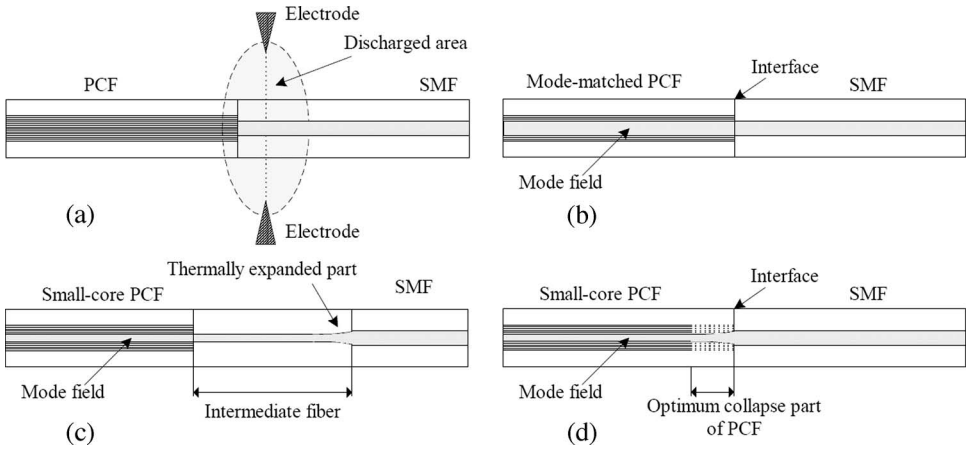

Fig. 3. (a) Splicing SMF to PCF with an offset of the joint to the central axis of arc discharge. (b) Splicing SMF to PCF having the same MFD. (c) Splicing SMF to a small-core PCF with an intermediate fiber. (d) Splicing SMF to a small-core PCF with an optimum mode field match at the interface.

the theoretical and experimental results indicates that the loss mechanism is due to the mode mismatch between PCF and SMF. For PCFs such as LMA-10 and HC-1550-02, which have similar MFDs as the SMFs, a low-loss splicing can be achieved when the splice does not alter the MFD of the PCF. However, for the small-core PCF having a much smaller MFD than the SMF, the splice loss is large, even when the air holes are kept intact, because of the mode field mismatch.

III. Principle of Low-Loss Splicing Between PCF and SMF

To avoid or minimize the air hole collapse in splicing PCF and SMF, an effective way is to choose a weaker fusion current and a shorter fusion time compared to the parameters of splicing SMF/SMF when fusion splicing PCF/SMF. However, a suitable arc energy should be obtained to soften the tips of the PCF and the SMF to achieve a good mechanical strength of the joint and at the same time minimize the collapse of air holes. Therefore, there is a tradeoff between the splice loss and the mechanical strength. Another important parameter is "overlap," which has not been paid much attention in previous research. "Overlap" means the overlap distance in which the two fibers are pushed further together because they have been softened as compared to when they merely touched each other in butt coupling. The tip part of the PCF is not softened enough when the arc discharge energy is low; therefore, a large overlap may cause bend misalignment when the two fibers are pushed together, thus increasing the coupling loss. Therefore, choosing a suitable overlap during splicing is also very important.

Because the softening point of the PCF is lower than that of the SMF, it is better to introduce a suitable offset [24], as shown in Fig. 3(a), between the joint and the central axis of the arc discharge, which will cause the arc discharge to weakly affect the tip of the PCF as compared with the tip of the SMF. This offset splicing method has two advantages. The first one is that it ensures a smaller amount of heat being applied to the PCF, and thus, it is easier to control the collapse of the air holes. The other is that it can balance the melting status by applying more heat to the SMF, because the SMF in general has a higher softening point than the PCF, as mentioned above.

For fusion splicing SMFs and PCFs having similar MFDs, a low-loss joint with good mechanical strength can be formed by choosing a suitably weak fusion current; short fusion time, offset, and overlap to minimize the collapse of air holes; and well melt two fibers together, as shown in Fig. 3(b). However, for splicing small-core PCFs and SMFs, the mode field mismatch can cause a large splice loss even when the air holes do not collapse. It is generally the practice to use an intermediate fiber as a bridge section between the two fibers to decrease the splice loss. Here, we will use a small-core fiber as an intermediate fiber, which will match the mode field of the small-core PCF when the core of the intermediate fiber is not expanded, and make a match with the SMF when the core is thermally treated to expand to have the same MFD of the SMF, as shown in Fig. 3(c). Another simpler solution we proposed in [22] is to control the degree of air hole collapse to realize low-loss splicing between a small-core PCF and an SMF without any intermediate fiber by repeated arc discharges. The principle of the method is to gradually control the collapse of the air holes of the PCF using a fusion splicer to obtain an enlarged mode field at the interface of the PCF that matches the mode field of the SMF, and at the same time to optimize the rate of hole collapse in the PCF to achieve an adiabatic mode field variation in the longitudinal direction to reduce the transition loss. To gradually collapse the holes in the PCF, repeated weak arc discharges with a short duration after an initial arc discharge are applied over the splice joint to achieve the optimum mode field match between the PCF and the SMF at the splice interface, as shown in Fig. 3(d). However, for small-core PCFs with high air-filling fraction, the mode field will not expand even when the air holes collapse; therefore, this method cannot be used in this kind of small-core PCFs, and we have to use an intermediate fiber to decrease the splice loss. We provide a detailed analysis of the various techniques in the next section.

IV. Low-Loss Fusion Splicing Experiments

After introducing the principle of low-loss splicing of SMFs and PCFs, we experimentally investigated the low-loss fusion splicing of different PCFs with SMF-28. First, the power of the 1550-nm source at the output of an SMF-28 fiber was measured.

Authorized licensed use limited to: IEEE Xplore. Downloaded on October 22, 2008 at 22:10 from IEEE Xplore. Restrictions apply.

TABLE III
OPTIMIZED PARAMETER OF SPLICING SMF-28 TO DIFFERENT FIBERS

Splice parameters	Fiber				
	SMF-28	LMA-10	HC-1550-02	LMA-5	PM-1550-01
Prefusion time	0.2 s	0.2 s	0.2 s	0.2 s	0.2 s
Prefusion current	10 mA	5 mA	5 mA	5 mA	5 mA
Gap	50 μm	50 μm	50 μm	50 μm	50 μm
Overlap	10 μm	5 μm	10 μm	3 μm	5 μm
Fusion time one	0.3 s	0	0	0	0
Fusion current one	10.5 mA	—	—	—	—
fusion time two	2.0 s	0.3 s	0.3 s	0.3 s	0.3 s
fusion current two	16.3 mA	12 mA	9 mA	10 mA	11 mA
fusion time three	2.0 s	0	0	0	0
fusion current three	12.5 mA	—	—	—	—
Center position	255	205	205	205	205
Number of repeated discharges	—	—	—	13	5

Then, the PCF with one end coupled to a power meter was spliced to the SMF-28 fiber to detect the coupling power. Next, the unspliced end of the PCF was subsequently spliced to another SMF-28 fiber in the same condition. Finally, the output power was again measured to observe splice reciprocity. The PCF was cleaved using a Furukawa S324 cleaver. The possibility of high-quality cleaving (a flat end face of the PCF) is above 90%. Because the tip of the PCF is not totally softened during splicing, any defect (such as a large cleave angle) will cause an extra splice loss and make the joint fragile, so the PCF with a flat end face must be chosen. It should be mentioned that in practical handling, the PCF cannot be cleaned with solvents after cleaving because the solvent will seep into the air holes of the PCF by capillary action, thus changing the light-guiding properties, which will result in a huge splice loss.

To compare the parameter set of PCF/SMF splicing with that of conventional SMF/SMF splicing, we first give the typical parameters of an Ericsson FSU-975 fusion splicer set for splicing two conventional SMFs. The parameters are listed in Table III. During prefusion, the fibers are cleared by low-level heating, and the main fusion process is fusion time two and fusion current two, which are the duration and magnitude of discharge current applied to the electrodes when the two fiber ends are pushed together [25].

In our experiments, to investigate the effect of arc discharge and easily perform discharge tests, we set fusion times one and three to zero, and then set fusion time two to 0.3 s and varied fusion current two. The prefusion current was set to 5.0 mA instead of 10 mA to avoid any heat collapse of the holes of the PCF before fusion splicing. We set the center position to 205, which corresponds to an offset distance of 50 μm. We chose a suitable overlap for different PCFs during fusion splicing. The other parameters are chosen to be the same as the parameters for splicing conventional fibers, and then, the two fibers are automatically aligned and spliced by the splicer.

A. *Splicing SMF to Solid-Core PCF With Similar MFDs*

The PCF LMA-10 and SMF-28 having similar MFDs were chosen to perform splicing experiments. We set the overlap to 5 μm and the fusion current time to 0.3 s and varied the fusion current from 9 to 14 mA with a step of 1 mA. The results are shown in Fig. 4. The splice losses are less than 0.4 dB when the fusion current is in the range of 10–13 mA. They are 0.36, 0.31, 0.19, and 0.23 dB for fusion currents of 10, 11, 12, and 13 mA, respectively. The corresponding splicing joints have good mechanical strength and can be bent in a circle with radii of about 6, 4, 1.8, and 1 cm, respectively, before breaking. The smallest splice loss (0.19 dB) was achieved when the fusion current was 12 mA. The corresponding splicing joint is shown

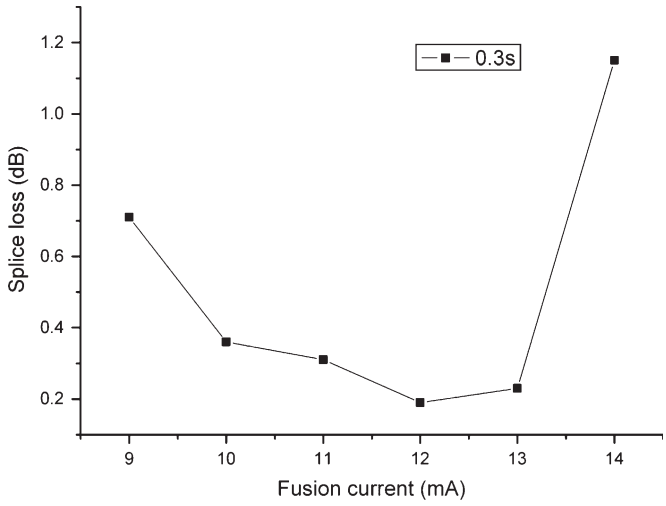

Fig. 4. Splice losses of SMF-28/LMA-10 as a function of the fusion current when the fusion time is fixed at 0.3 s. The offset and overlap are 50 and 5 μm, respectively.

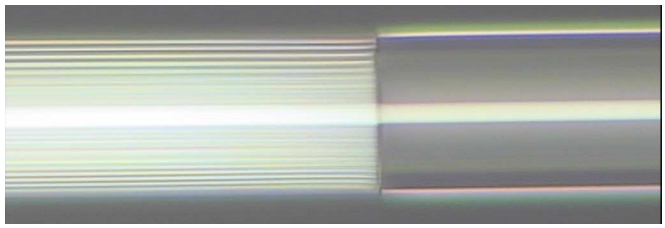

Fig. 5. Optical microscopy image of the fusion joint of LMA-10/SMF-28 when the splice loss is 0.19 dB.

Authorized licensed use limited to: IEEE Xplore. Downloaded on October 22, 2008 at 22:10 from IEEE Xplore. Restrictions apply.

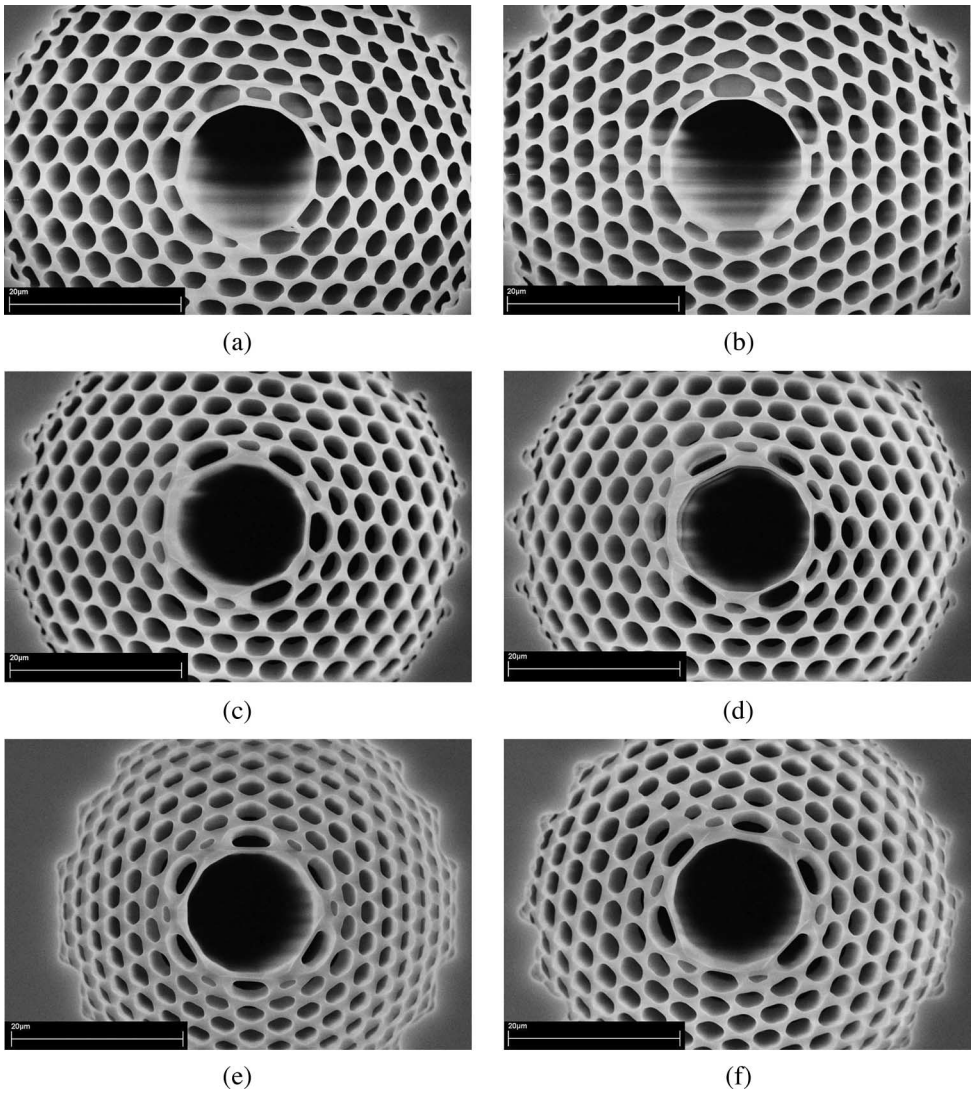

Fig. 6. End views of HC-1550-02 with different fusion currents when the fusion time was fixed at 0.3 s and the offset was fixed at 50 μm. (a) 9 mA. (b) 9.5 mA. (c) 10 mA. (d) 10.5 mA. (e) 11 mA. (f) 11.5 mA.

in Fig. 5. We can observe that there is no visible difference of air hole structures between the spliced region of the LMA-10 and the region far away from the splice joint, which means that a low-loss splicing joint was formed because the air hole collapse was largely avoided. Statistically, ten splices were done that yielded an average splice loss of 0.32 dB with a standard deviation of 0.07 dB. The splice loss from LMA-10 to SMF-28 was 0.30 dB. The loss difference in two opposite directions is within the deviation; thus, the splice is optical reciprocal.

B. Splicing SMF to Hollow-Core PCF With Similar MFDs

The low-loss fusion splicing between a hollow-core PCF (also called PBG fiber) and an SMF is more difficult [15]–[17], and only one paper [17] has recently provided details on the fusion process and fusion parameters. Here, we first investigate the effect of the fusion current on the collapse of the air holes of a hollow-core PCF and then measure the splice loss for different values of fusion current.

The hollow-core PCF HC-1550-02 and SMF-28 having similar MFDs were chosen to perform the experiments. Because the hollow-core PCF more readily reaches its softening point, and its central region caves in [16], [26] due to surface tension, we set the overlap to 10 μm to obtain a good mechanical strength when fusion splicing. We fixed the fusion time to 0.3 s and changed the fusion current from 9 to 11.5 mA in steps of 0.5 mA. By withdrawing SMF-28 just before the start of the arc discharge, the tip of the HC-1550-02 was not spliced to the SMF-28 but heated by the arc discharge so that we could check the degree of air collapse. Fig. 6 shows the SEM images of the end face of HC-1550-02 when the fiber was subjected to an arc discharge from various fusion currents. We can observe that the collapse of the cladding holes is proportional to the fusion current. Because of the high air-filling fraction of the air–silica cladding, there is a thermal gradient when the heat transfers from the solid silica ring cladding to the center of the holey region [26]. When the fusion current is 9 mA, only the first outer air holes partially collapse. When the fusion current is increased to 10 mA, two outer air holes collapse. Fusion

Authorized licensed use limited to: IEEE Xplore. Downloaded on October 22, 2008 at 22:10 from IEEE Xplore. Restrictions apply.

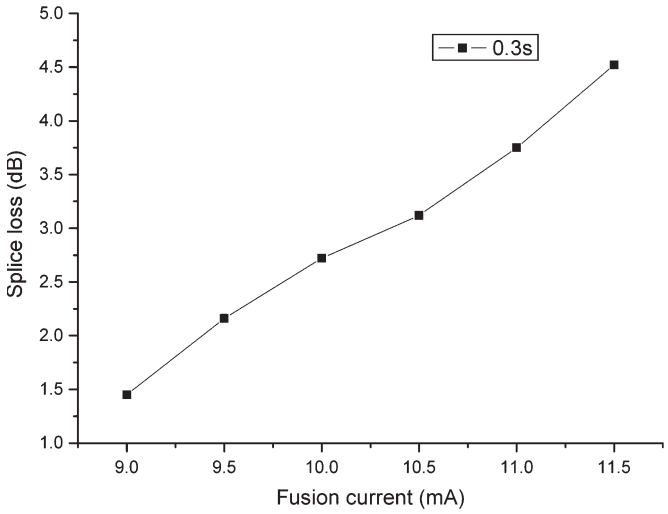

Fig. 7. Splice losses of SMF-28/HC-1550-02 measured versus the fusion current with fixed fusion time of 0.3 s. The offset and overlap are 50 and 10 μm, respectively.

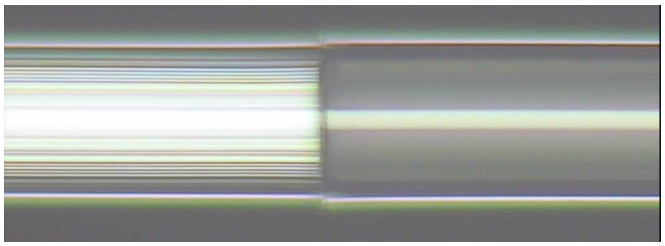

Fig. 8. Optical microscopy image of the fusion joint of HC-1550-02/SMF-28 with splice loss of 1.45 dB.

currents of 11 and 11.5 mA correspond to the collapse of three and four outer air holes, respectively. The further collapse of air holes with increasing fusion current is demonstrated in [26]. The surface tension also makes the central air–silica region cave in, and the degree of recess of the end part of the PCF is proportional to the fusion current. The splice loss was increased when the fusion current increased from 9 to 11.5 mA, as shown in Fig. 7. The increasing splice loss with the fusion current is due to two reasons: One is that distorting the periodic air–silica cladding structure will increase the confine loss at the splice joint, and the other is that the increasing recess that created an air gap between two fiber cores will increase the coupling loss because the light coming out from the SMF will quickly expand when there is an air gap. The lowest splice loss (1.45 dB) was achieved when the fusion current was 9 mA. The corresponding splicing joint, which is shown in Fig. 8, had good mechanical strength and could be bent to a radius of about 2.5 cm before breaking. The splicing result is of the same order of the best result reported [16] and only needs one arc discharge. From Fig. 8, we cannot observe a visible collapse when we compare the spliced and unspliced region of the PCF. Thus, we have demonstrated that a low-loss splicing between a hollow-core PCF and an SMF can be achieved even with a single arc discharge when we choose suitable parameters. Ten splices were done using the above method that yielded an average splice loss of 1.87 dB with a standard deviation of 0.18 dB in the range of 1.45–2.01 dB. The splice loss from HC-1550-02 to SMF-28 was 2.48 dB; thus, the difference of the splice losses in two opposite directions is significantly large. It is because the higher order modes were excited in HC-1550-02, which cannot couple well to SMF-28 [17].

C. Splicing SMF to Small-Core PCF With Low Air-Filling Fraction

In [27], Frazão *et al.* achieved low-loss splicing between a small-core PCF (NL- 2.3-1555) and an SMF-28 using a fusion splicer. However, the authors did not give a proper explanation about the results because low-loss splicing cannot be achieved due to the mode field mismatch when the air holes of the small-core PCF are not collapsed, as explained earlier. In [22], we first provided a simple method to splice small-core PCFs to SMFs by repeated arc discharges. Part of the contents of [22] will be included here for completeness. The mechanism of microhole collapse in these kinds of small-core PCFs, the mechanical strength of the splicing joint, and the limits of this method are further discussed.

In our experiments, the small-core PCF we chose to splice to SMF-28 was LMA-5. We set the overlap to 1 μm and the offset to 50 μm and fixed the fusion time at 0.3 s. To illustrate the degree of air hole collapse, we first observed the end face of LMA-5 by SEM after various arc discharges. The fusion current used was 10.0 mA. By withdrawing the SMF just before the start of the arc discharge (the method we mentioned above), we can observe the collapse of the end face of the PCF as a result of the arc discharge. We repeatedly applied arc discharges with the same power to heat the LMA-5. Fig. 9(a)–(d) shows the SEM images of the LMA-5 end face after two, five, seven, and nine discharges, respectively; the time gap between two consecutive discharges is 2 s. We observed that the average hole diameter was 0.83 μm when the number of arc discharges was two, the holes shrunk to 0.70 and 0.24 μm after five and seven discharges, and almost all the holes are closed after nine discharges. We found that the microhole collapse of LMA-5 was quite different from the collapse of HC-1550-02. All the holes shrunk at the same rate, and there was almost no recess in the air–silica region. This is because heat can quickly transfer in the low air-filling-fraction air–silica structure; thus, no significant thermal gradient exists in the PCF's cross section. Moreover, because the solid silica part, of which most of the air–silica cladding is made, can sustain the air–silica structure when the air holes shrink, the end surface of the PCF will not cave in when exposed to heat during splicing.

We then performed fusion splicing between LMA-5 and SMF-28. The splice losses measured for light propagating from SMF-28 to LMA-5, as functions of the number of discharges and the fusion current, are shown in Fig. 10. It can be seen from Fig. 10 that, for fusion currents of 9.5, 10.0, and 11 mA, the minimum splice loss of 1.11, 0.90, and 1.80 dB can be obtained after 23, 13 and four arc discharges. Fig. 11 shows the side view of the splicing joint with 10.0-mA discharge current after 13 discharges. We can clearly observe that the holes of the LMA-5 have gradually collapsed to a certain degree, which results in an enlarged mode field in the PCF that optimized the mode field match between the two fibers and, hence, minimized

Authorized licensed use limited to: IEEE Xplore. Downloaded on October 22, 2008 at 22:10 from IEEE Xplore. Restrictions apply.

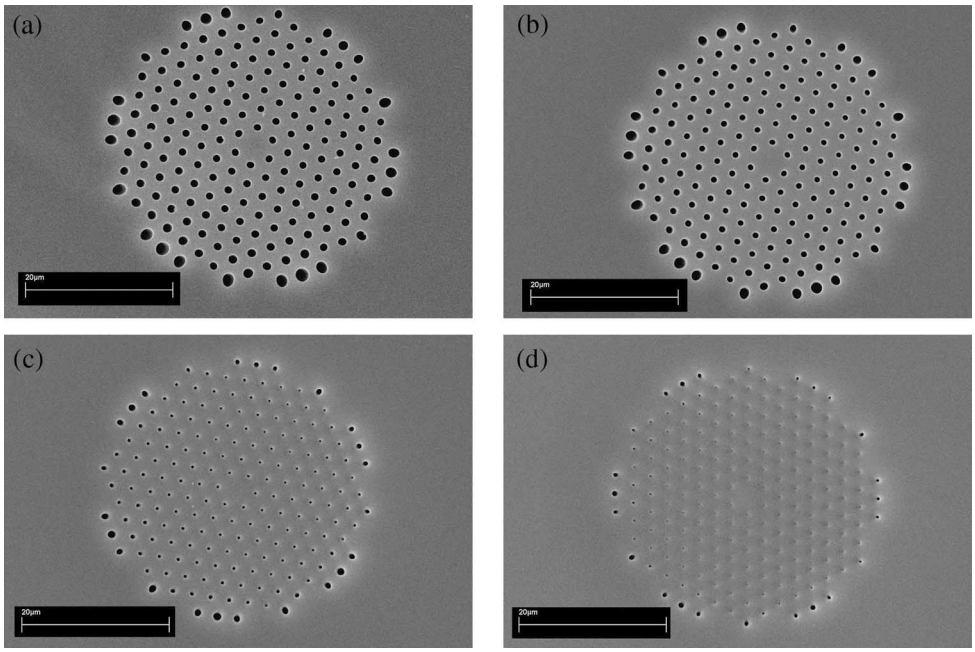

Fig. 9. End views of LMA-5 after (a) two, (b) five, (c) seven, and (d) nine discharges. The fusion time, current, and offset are 0.3 s, 10 mA, and 50 μm, respectively.

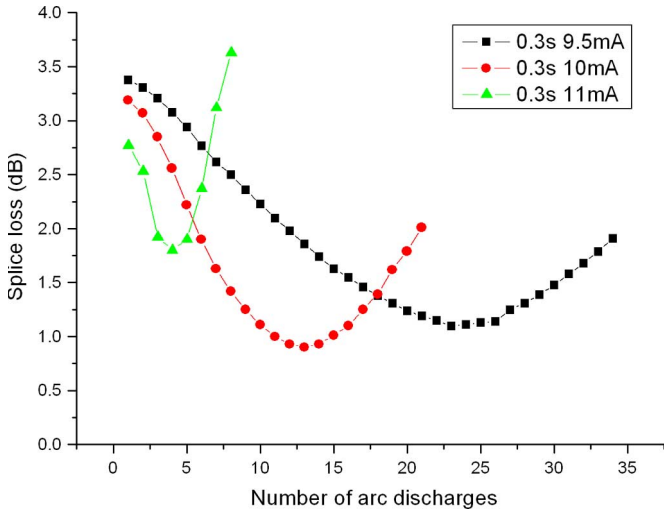

Fig. 10. Splice losses of SMF-28/LMA-5 as a function of the number of arc discharges with fusion current as a parameter. The fusion time, offset, and overlap are 0.3 s, 50 μm, and 1 μm, respectively.

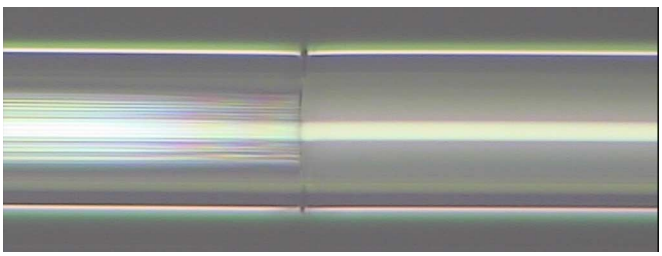

Fig. 11. Optical microscopy image of the fusion joint of LMA-5/SMF-28 with splice loss of 0.90 dB.

the splice loss. Five splices were done, and the measured loss was in the range of 0.90–1.41 dB that yielded an average splice loss of 1.14 dB with a standard deviation of 0.18 dB. The splice loss from LMA-5 to SMF-28 was 1.09 dB, which proved that it has good splice reciprocity. The mechanical strength was not very good; the bending radius was about 10 cm before the fibers broke when the overlap was 1 μm. However, the splicing joint can be bent in a circle with a minimum radius of about 2 cm before breaking when the overlap changed to 3 μm, with the splice loss still being approximately the same. The minimum experimental loss (0.90 dB) obtained may be caused by the nonperfect mode field mismatch at the PCF/SMF interface and by the mode field expansion (transition) loss in the gradual hole-collapsing part of the small-core PCF. Because of the short transition length, as can be observed from the side views of the collapsed region in Fig. 11, the mode field transition loss may not be neglected. We believe that the splice loss could be further reduced by using a wider electrode gap to optimize the transition length [28]. The same method was used to splice SMF-28/NL-1550-POS-1, and the minimum loss was significantly less than the butt-coupling loss [22]. Five splices were done when the fusion current was 9.5 mA, which yielded an average splice loss of 1.61 dB with a standard deviation of 0.37 dB. The splicing joint can be bent in a circle with a minimum radius of about 2 cm when the overlap is 3 μm. The standard deviation of the experimental losses of the splicing between SMF-28/NL-1550-POS-1 was larger than that of SMF-28/LMA-5. This might be caused by the aberration of the transverse alignment because the smaller core is more sensitive to misalignment when the two fibers are automatically aligned and spliced.

The small-core PCFs that we have successfully tested have low air-filling fraction cladding, and thus, the guiding mode of this kind of small-core PCFs pervades into the air–silica cladding; hence, the MFD is generally larger than the diameter of the solid core. When the microholes shrink, the guiding mode can expand, and the end surface of the collapsed PCF keeps

Authorized licensed use limited to: IEEE Xplore. Downloaded on October 22, 2008 at 22:10 from IEEE Xplore. Restrictions apply.

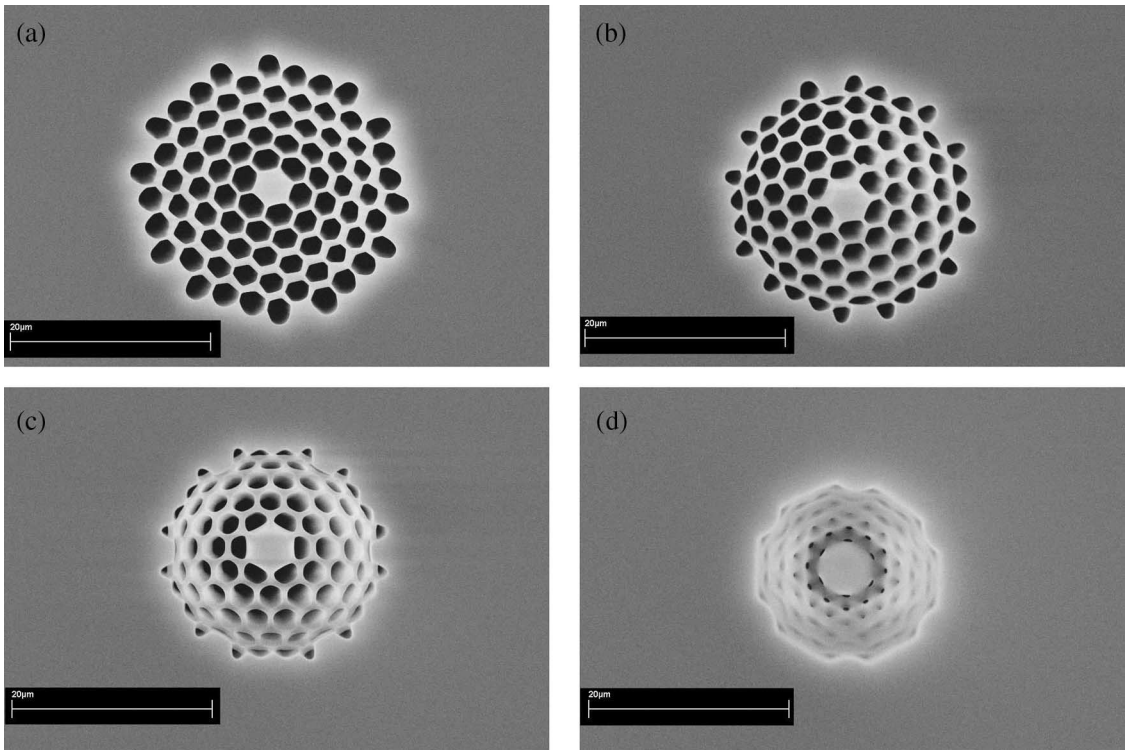

Fig. 12. End views of NL-3.3-880 with different fusion currents when the fusion time was fixed at 0.3 s and the offset was fixed at 50 μm. (a) 12 mA. (b) 13 mA. (c) 14 mA. (d) 14.5 mA.

flat, which contributes to the low-loss splice of this kind of PCF to the SMF. However, this method cannot be used to improve the coupling efficiency between the SMF and the small-core PCF with high air-filling fraction, as will be discussed in the next part.

D. Splicing SMF to Small-Core PCF With High Air-Filling Fraction

The small-core PCF with high air-filling fraction generally has about 90% air-filling ratio in the air–silica cladding region. For this kind of small-core PCF, the function of the air–silica cladding is to support the extremely small silica core with a very low refractive index (just over 1) medium. The optical properties of the core closely resemble those of a glass microrod suspended in the air, which results in the strong confinement of the light and a large nonlinear coefficient. The MFD of this kind of small-core PCF is generally smaller than the diameter of the core. The small-core PCF we chose in our experiment was NL-3.3-880.

To explore the microhole collapse property of this kind of small-core PCF, the same method as in Section IV-B (withdraw the SMF before the start of arc discharge) was used. Fig. 12 shows the end views of NL-3.3-880 when the fiber was subjected to an arc discharge from 12 to 14.5 mA. We can observe that the collapse of the cladding holes of NL-3.3-880 is similar to that of the hollow-core PCF. When the fusion current is 14 mA, two outer air holes totally collapse, but three inner air holes are still open, as shown in Fig. 12(c). The guiding light is still strongly confined to the small core by the inner six holes around the core rather than pervading into the air–silica cladding. This does not give rise to an increase in the MFD of the PCF; thus, the partial collapse of air holes in this kind of small-core PCF does not improve the coupling efficiency. Furthermore, the central part of the small-core PCF caves in when air holes collapse because of the high air-filling fraction of the air–silica cladding. Consequently, just like the hollow-core PCF, the air gap between the two fibers gives rise to an increase in the splice loss due to the cavein. When the fusion current increases to 14.5 mA, the inner air holes shrink to about 0.4 μm, as shown in Fig. 12(d). At this time, the mode field expands; however, the degree of recess also increases, so it is hard to judge whether the partial collapse can be of benefit to the coupling efficiency. The experiments, by repeated arc discharges, were then done, as shown in Fig. 13. The splice losses increased with the number of arc discharges, which proves that the partial collapse of air holes cannot improve the coupling efficiency, and the recess of the end face of the PCF increases the coupling loss. After 11 arc discharges with a fusion current of 13 mA, the splice loss increased from 8.58 to 10.74 dB. As shown in Fig. 14(a), the recess part of the PCF is clearly visible from the side view.

Because partial collapse cannot be used to splice the small-core PCF with high air-filling fraction to the conventional SMF, another method that uses an intermediate fiber to solve the mode mismatch problem should be utilized, as mentioned in Section III. Here, we use the fiber UHNA3 from Nufern as the intermediate fiber. The MFD and the Numerical aperture of UHNA3 at 1550 nm are about 4.1 μm and 0.35. The theoretical losses of UHNA3/SMF-28 and UHNA3/NL-3.3-880 are about

Authorized licensed use limited to: IEEE Xplore. Downloaded on October 22, 2008 at 22:10 from IEEE Xplore. Restrictions apply.

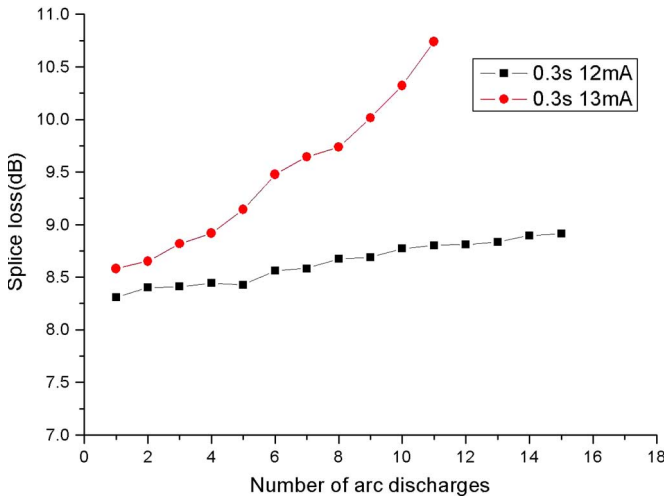

Fig. 13. Splice losses of SMF-28/NL-3.3-880 as a function of the number of arc discharges with fusion current as a parameter. The fusion time, offset, and overlap are 0.3 s, 50 μm, and 5 μm, respectively.

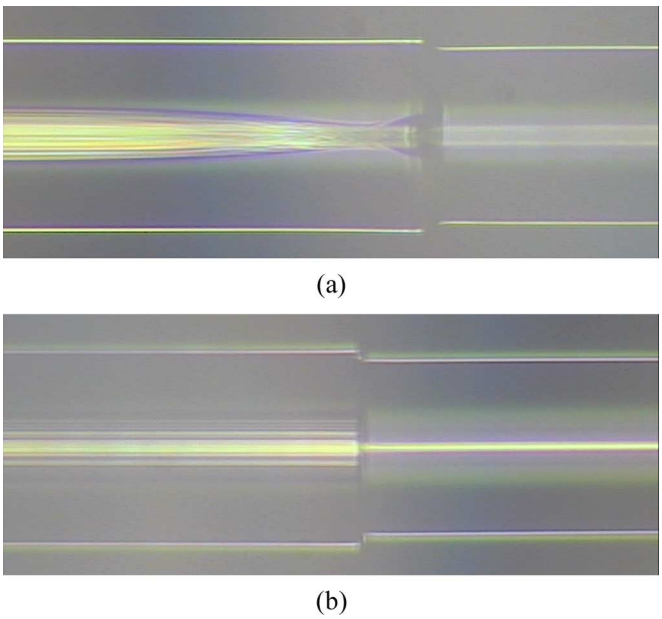

Fig. 14. Optical microscopy images of the fusion joints of (a) NL-3.3-880/SMF-28 with the splice loss 10.74 dB and (b) NL-3.3-880/UHNA3 with the splice loss 1.93 dB.

3.32 and 1.58 dB, respectively, according to (2). UHNA3 has a thermally expanded core (TEC), thus making it possible for the mode field to expand so that it matches the mode field of SMF-28 when suitable heating is applied by the fusion splicer. The TEC technology for conventional mode mismatch fibers such as erbium-doped fibers has been widely used, and the fusion splicer has the splice parameter set for this operation. We used Program 06 of Ericsson FSU-975 to splice SMF-28 to UHNA3 and to achieve a splice loss of about 0.60 dB, and then, we spliced UHNA3 to NL-3.3-880 without collapsing the air holes using the same method described in Section IV-A. The splice joint of UHNA3/NL-3.3-880 is shown in Fig. 14(b), which corresponds to a loss of about 1.93 dB, which is a

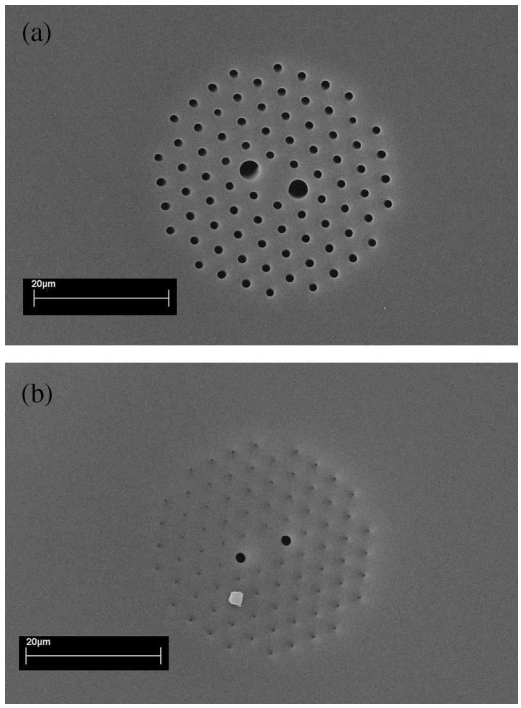

Fig. 15. End views of PM-1550-01 with different fusion currents when the fusion time was fixed at 0.3 s, and the offset was fixed at 50 μm. (a) 12 mA. (b) 13 mA.

little larger than the butt-coupling loss. We can conclude that the total splice loss can decrease to about 2.53 dB using an intermediate fiber.

E. Splicing SMF to Polarization-Maintaining PCF

The polarization-maintaining PCF that we used in our experiments was PM-1550-01, which has different microhole sizes in two perpendicular transverse directions. Because the air-filling fraction of PM-1550-01 is not high, the nature of its hole collapse is similar to the small-core PCF with low air-filling fraction, so the partial collapse of air holes can increase the coupling efficiency when the MFD of PM-PCF is smaller than that of the conventional fiber. However, because the rate of hole collapse is almost same, and the size of microholes is rather different, the larger holes still open when the small holes collapse to close, as shown in Fig. 15. Fig. 15 shows the end views of PCF-1550-01 when the fusion currents are 12 and 13 mA. Therefore, the expanded mode field in two perpendicular transverse directions will be more different, which will limit the improvement of the coupling efficiency between PM-1550-01 and SMF-28 when repeated weak arc discharges are applied. For splicing SMF-28/PM-1550-01 (Fig. 16), when the fusion currents were 10 and 11 mA, minimum splice losses of 2.08 and 2.03 dB were obtained after 18 and five discharges, respectively. The splice loss from PM-1550-01 to SMF-28 in the same condition was about 1.80 dB, which is almost splice reciprocity. When the fusion current was 12 mA, the minimum splice loss was 2.41 dB after the first discharge; further discharges increased the splice loss. The structure of the splicing joint when the loss is 2.03 dB is shown in Fig. 17.

Authorized licensed use limited to: IEEE Xplore. Downloaded on October 22, 2008 at 22:10 from IEEE Xplore. Restrictions apply.

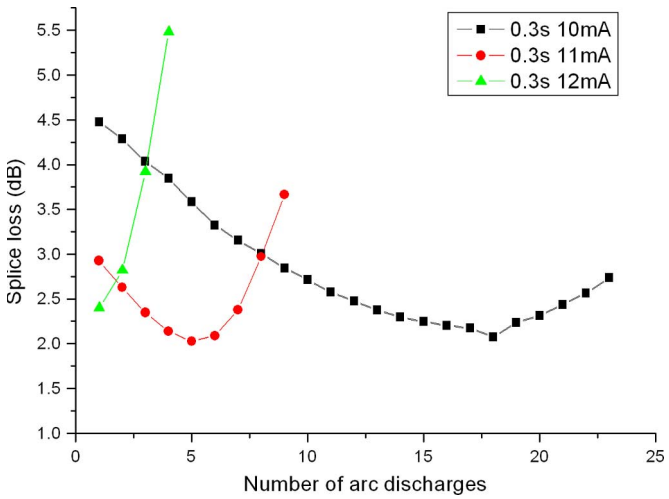

Fig. 16. Splice losses of SMF-28/PM-1550-01 as a function of the number of arc discharges with fusion current as a parameter. The fusion time, offset, and overlap are 0.3 s, 50 μm, and 5 μm, respectively.

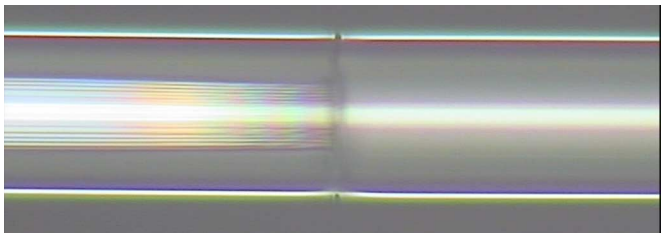

Fig. 17. Optical microscopy image of the fusion joint of PM-1550-01/SMF-28 with splice loss of 2.03 dB.

We can observe that the air holes gradually collapse toward the splicing interface, as we expected. When we set the overlap to 5 μm, five splices were done when the fusion current was 11 mA, which yielded an average splice loss of 2.22 dB with a standard deviation of 0.22 dB, and the splicing joint can be bent in a circle of about 1.5 cm before breaking. The splice loss significantly decreased compared with the splice loss when butt coupled. However, the experimental loss of SMF-28/PM-1550-01 was larger than that of SMF-28/LMA-5. This is because the mode field shape difference between PM-1550-01 and SMF-28 will lead to an extra loss in addition to the transition loss.

V. Conclusion

In conclusion, we have investigated the microhole collapse property of five different kinds of PCFs by observing the side views of PCFs using an optical microscopy and the end views of PCFs using an SEM after splicing. The physical mechanism of the splice loss was studied in detail, and then, different methods were proposed according to the different structure of PCFs to achieve low-loss splicing. A precise alignment and a proper heat energy being applied to the joint of PCF/SMF were the keys to achieving low-loss splicing so that changing the fusion current or changing the fusion time in a suitable range can lead to optimum results. For the PCF and the SMF having similar MFDs, low-loss splicing can be achieved by minimizing the collapse of air holes of the PCF. For the small-core PCF with low air-filling fraction, including the PM-PCF, a low-loss splicing can be achieved by applying repeated arc discharges over the splicing joint to gradually collapse the air holes of the small-core PCF. For the small-core PCF with high air-filling fraction, an intermediate fiber should be used to decrease the splice loss. We have demonstrated the low-loss splice of these different PCFs with conventional SMFs. The optimized splice results and splice parameters are listed in Tables II and III, respectively. We believe that the results can be further improved by using a fusion splicer that has an higher precision in alignment and in controlling the fusion energy. The experimental results prove that fusion splicing is a simple and practical solution to solve the coupling problem between PCFs and SMFs, which will benefit the development of different PCF devices and sensors in practical application.

Acknowledgment

The authors would like to thank Prof. H. Y. Tam, Dr. W. S. Man, Dr. H. L. Ho, Dr. W. H. Chung, and Dr. A. Zhang for providing the equipment and for useful discussion.

References

[1] J. C. Knight, "Photonic crystal fibres," *Nature*, vol. 424, no. 6950, pp. 847–851, Aug. 2003.
[2] P. Russell, "Photonic crystal fibers," *Science*, vol. 299, no. 5605, pp. 358–362, Jan. 2003.
[3] P. Russell, "Photonic-crystal fibers," *J. Lightw. Technol.*, vol. 24, no. 12, pp. 4729–4749, Dec. 2006.
[4] J. C. Knight, T. A. Birks, P. S. J. Russell, and D. M. Atkin, "All-silica single-mode optical fiber with photonic crystal cladding," *Opt. Lett.*, vol. 21, no. 19, pp. 1547–1549, Oct. 1996.
[5] P. J. Bennett, T. M. Monro, and D. J. Richardson, "Toward practical holey fiber technology: Fabrication, splicing, modeling, and characterization," *Opt. Lett.*, vol. 24, no. 17, pp. 1203–1205, Sep. 1999.
[6] J. T. Lizier and G. E. Town, "Splice losses in holey optical fibers," *IEEE Photon. Technol. Lett.*, vol. 13, no. 8, pp. 794–796, Aug. 2001.
[7] Y. L. Hoo, W. Jin, J. Ju, and H. L. Ho, "Loss analysis of single-mode fiber/photonic-crystal fiber splice," *Microw. Opt. Technol. Lett.*, vol. 40, no. 5, pp. 378–380, 2004.
[8] K. Nakajima, K. Hogari, J. Zhou, K. Tajima, and I. Sankawa, "Hole-assisted fiber design for small bending and splice losses," *IEEE Photon. Technol. Lett.*, vol. 15, no. 12, pp. 1737–1739, Dec. 2003.
[9] C. Kerbage, A. Hale, A. Yablon, R. S. Windeler, and B. J. Eggleton, "Integrated all-fiber variable attenuator based on hybrid microstructure fiber," *Appl. Phys. Lett.*, vol. 79, no. 19, pp. 3191–3193, Nov. 2001.
[10] B. Bourliaguet, C. Paré, F. Émond, A. Croteau, A. Proulx, and R. Vallée, "Microstructured fiber splicing," *Opt. Express*, vol. 11, no. 25, pp. 3412–3417, Dec. 2003.
[11] B. H. Park, J. Kim, U. C. Paek, and B. H. Lee, "The optimum fusion splicing conditions for a large mode area photonic crystal fiber," *IEICE Trans. Electron.*, vol. E88-C, no. 5, pp. 883–888, 2005.
[12] J. H. Chong, M. K. Rao, Y. Zhu, and P. Shum, "An effective splicing method on photonic crystal fiber using CO_2 laser," *IEEE Photon. Technol. Lett.*, vol. 15, no. 7, pp. 942–944, Jul. 2003.
[13] J. H. Chong and M. K. Rao, "Development of a system for laser splicing photonic crystal fiber," *Opt. Express*, vol. 11, no. 12, pp. 1365–1370, Jun. 2003.
[14] A. D. Yablon and R. T. Bise, "Low-loss high-strength microstructured fiber fusion splices using GRIN fiber lenses," *IEEE Photon. Technol. Lett.*, vol. 17, no. 1, pp. 118–120, Jan. 2005.
[15] T. P. Hansen, J. Broeng, C. Jakobsen, G. Vienne, H. R. Simonsen, M. D. Nielsen, P. M. W. Skovgaard, J. R. Folkenberg, and A. Bjarklev, "Air-guiding photonic bandgap fibers: Spectral properties, macrobending loss, and practical handling," *J. Lightw. Technol.*, vol. 22, no. 1, pp. 11–15, Jan. 2004.

Authorized licensed use limited to: IEEE Xplore. Downloaded on October 22, 2008 at 22:10 from IEEE Xplore. Restrictions apply.

[16] F. Benabid, F. Couny, J. C. Knight, T. A. Birks, and P. S. J. Russell, "Compact, stable and efficient all-fibre gas cells using hollow-core photonic crystal fibres," *Nature*, vol. 434, no. 7032, pp. 488–491, Mar. 2005.
[17] R. Thapa, K. Knabe, K. L. Corwin, and B. R. Washburn, "Arc fusion splicing of hollow-core photonic bandgap fibers for gas-filled fiber cells," *Opt. Express*, vol. 14, no. 21, pp. 9576–9583, Oct. 2006.
[18] W. Wadsworth, A. Witkowska, S. Leon-Saval, and T. Birks, "Hole inflation and tapering of stock photonic crystal fibres," *Opt. Express*, vol. 13, no. 17, pp. 6541–6549, Aug. 2005.
[19] J. K. Chandalia, B. J. Eggleton, R. S. Windeler, S. G. Kosinski, X. Liu, and C. Xu, "Adiabatic coupling in tapered air–silica microstructured optical fiber," *IEEE Photon. Technol. Lett.*, vol. 13, no. 1, pp. 52–54, Jan. 2001.
[20] S. G. Leon-Saval, T. A. Birks, N. Y. Joly, A. K. George, W. J. Wadsworth, G. Kakarantzas, and P. S. J. Russell, "Splice-free interfacing of photonic crystal fibers," *Opt. Lett.*, vol. 30, no. 13, pp. 1629–1631, Jul. 2005.
[21] L. M. Xiao, W. Jin, M. S. Demokan, H. L. Ho, H. Y. Tam, J. Ju, and J. Yu, "Photopolymer microtips for efficient light coupling between single-mode fibers and photonic crystal fibers," *Opt. Lett.*, vol. 31, no. 12, pp. 1791–1793, Jun. 2006.
[22] L. M. Xiao, W. Jin, and M. S. Demokan, "Fusion splicing small-core photonic crystal fibers and single-mode fibers by repeated arc discharges," *Opt. Lett.*, vol. 32, no. 2, pp. 115–117, Jan. 2007.
[23] A. D. Yablon, *Optical Fiber Fusion Splicing*. Heidelberg, Germany: Springer-Verlag, 2005.
[24] J. C. Fajardo, M. T. Gallagher, and Q. Wu, "Splice joint and process for joining a microstructured optical fiber and a conventional optical fiber," U.S. Patent 20 030 081 915 A1, May 1, 2003.
[25] *User's Manual for the FSU 975 Single Fiber Fusion Splicer by Ericsson*.
[26] L. M. Xiao, W. Jin, M. S. Demokan, H. L. Ho, Y. L. Hoo, and C. L. Zhao, "Fabrication of selective injection microstructured optical fibers with a conventional fusion splicer," *Opt. Express*, vol. 13, no. 22, pp. 9014–9022, Oct. 2005.
[27] O. Frazão, J. P. Carvalho, and H. M. Salgado, "Low-loss splice in a microstructured fibre using a conventional fusion splicer," *Microw. Opt. Technol. Lett.*, vol. 46, no. 2, pp. 172–174, 2005.
[28] H. Y. Tam, "Simple fusion splicing technique for reducing splicing loss between standard single mode fibres and erbium-doped fibre," *Electron. Lett.*, vol. 27, no. 17, pp. 1597–1599, Aug. 1991.

Limin Xiao received the B.S. degree in measurement and control technology and instrumentation from Wuhan University, Wuhan, China, in 2001 and the M.S. degree in optical engineering from Tsinghua University, Beijing, China, in 2004. He is currently working toward the Ph.D. degree in electrical engineering at the Hong Kong Polytechnic University, Kowloon, Hong Kong.

His research interests include fiber-optic sensors and devices. His current research is focused on the low-loss splicing of different photonic crystal fibers, microfabrication of fiber devices, developing hybrid photonic crystal fiber devices, and the design and simulation of novel photonic crystal fiber structures.

Mr. Xiao is a Student Member of the Optical Society of America and The International Society for Optical Engineers.

M. S. Demokan (SM'89) received the B.Sc. degree in electronic engineering from the Middle East Technical University, Ankara, Turkey, in 1970, and the M.Sc. and Ph.D. degrees in electronic engineering from King's College, University of London, London, U.K., in 1972 and 1976, respectively.

Between 1976 and 1983, he was with the Middle East Technical University, where he served various capacities, including Dean of Faculty, Head of Department, and Associate Professor. After conducting research for a year as a Visiting Senior Research Fellow with Imperial College, University of London, he joined the Hirst Research Center, General Electric Company, Wembley, U.K., in 1984, where he directed contract research as the Head of the Department of Optoelectronic Components and as the Chief Scientist of the Department of Optical Communications. Since 1988, he has been with the Hong Kong Polytechnic University, Kowloon, Hong Kong, where he was promoted to Chair Professor in 1992. He was the Head of the Department of Electrical Engineering between 1988 and 1995, the Dean of the Faculty of Engineering between 1995 and 2000, the Associate Vice-President between 1997 and 2000, and the Vice-President overseeing university research and academic appointments and promotion between 2000 and 2003. He has been the Vice-President responsible for academic development since 2005. He is the author of two books and more than 180 refereed papers. His current research interests include optical communication systems (especially all-optical switching and photonic crystal fibers) and various types of optical sensors.

Prof. Demokan is a Fellow of the Hong Kong Institution of Engineers and the Institution of Electrical Engineers (U.K.). He served on the Editorial Board of two international journals, organized various international conferences, and served in various capacities in professional bodies.

Wei Jin (M'95–SM'98) received the B.Eng. and M.Sc. degrees from Beijing University of Aeronautics and Astronautics, Beijing, China, in 1984 and 1987, respectively, and the Ph.D. degree in fiber optics from the University of Strathclyde, Glasgow, U.K., in 1991.

From 1991 to 1995, he was a Postdoctoral Research Fellow with the University of Strathclyde. Since 1996, he has been with the Hong Kong Polytechnic University, Kowloon, Hong Kong, where he is currently a Full Professor. He authored or coauthored two books and over 300 journals and conference proceeding publications and is the holder of five patents, all in the area of fiber-optic devices and sensors.

Prof. Jin is a member of The International Society for Optical Engineers and the Optical Society of America. He received the President Award of the Hong Kong Polytechnic University for outstanding performance in research and scholarly activities. He secured research funds of over HK $25 million over the past several years.

Yiping Wang, photograph and biography not available at the time of publication.

Chun-Liu Zhao received the B.S. degree in applied physics from Inner Mongolia University, Huhhot, China, and the M.S. and Ph.D. degrees in optics from Nankai University, Tianjin, China, in 1999 and 2002, respectively.

From 2002 to 2004, she was a Research Fellow with the Lightwave Department, Institute for Infocomm Research, Singapore. From 2004 to 2007, she was a Postdoctoral Fellow with the Electrical Engineering Department, Hong Kong Polytechnic University, Kowloon, Hong Kong. She is currently a Professor with the School for Information and Optoelectronics Science and Engineering, South China Normal University, Guangzhou, China. Her research interests include fiber grating, optical fiber amplifiers and lasers, and applications based on photonic crystal fibers.

Authorized licensed use limited to: IEEE Xplore. Downloaded on October 22, 2008 at 22:10 from IEEE Xplore. Restrictions apply.